HEORETICAL AND EXPERIMENTAL INVESTIGATION ON STATIC AND DYNAMIC BEHAVIOR OF ROTATING MACHINERY+

Mustafa K Issa* **Hassan H Mahdi****

Safaa H Abdulrahman***

Abstract

This study is concerned with the static and dynamic characteristics of solid shaft supported by bearing with and without number of discs situated along the shaft. The effects of including and disregarding gyroscopic, axial load, translation mass and rotation mass inertia on the natural frequencies and deflection at the disc position have been studed. The finite beam element model with four degrees of freedom at each node is used in this study, and a special computer programming was developed for the problem. Experimental work was carried out on a number of discs arranged along the shaft length, and the obtained results are compared with theoretical ones, which show good agreements.

This work and technique have shown good agreement with those of other investigators, and the computer program developed in this study proves to be quite efficient and can be used in the analysis of such systems.

المستخلص

هذا البحث يهتم بدراسة الخواص السكونية والحركية للمحاور الصلدة الدوارة المرتكزة على محامل مرنة مع عدد من الاقراص او بدونها والموزعة على طول المحور. تم في هذا البحث دراسة تأثيرات الأخذ بنظر الاعتبار أو اهمال القوى التوازنية، الحمل المحوري، الكتل الافقية والكتل الدورانية على الترددات الطبيعية للمحور والتشوه في موقع القرص.

استخدم في هذا البحث طريقة العناصر المحددة (عنصر العتبة) وباربعة درجات حرية لكل عقدة من العنصر، كذلك تم تطوير برنامج حاسوب خاص لحل هذه المشاكل، للحصول على النتائج المطلوبة. تم اجراء تجارب عملية لعدد من الاقراص رتبت على طول المحور وقورنت بالنتائج النظرية وكان هناك تقارب جيد بينها.

هذا العمل والتقنية قد اعطى نتائج جيدة مقارنة مع باحثين اخرين، كما ان برنامج الحاسوب الذي تم تطويره في هذه الدراسة أثبت كفائته ويمكن استخدامه لتحليل مثل هذه الانظمة.

Introduction

Complex rotor systems have broad industrial applications, such as steam and gas turbine, turbo-generators, reciprocating and centrifugal compressors, internal combustion engines, grinds, milling and aerospace machines. Flexible rotating shafts are employed in these

+Received on ١/٤/٢٠٠٧ Accepted on 1/10/2007

* Lecturer/ Al Mustansirya University

** Lecturer/ Technical College Baghdad

*** Asst. Prof./ University of Technology

machines for efficient power transmission, high speed transportation and cost effective operation. The vibration of these flexible components is a major concern in optimal design of complex rotor system. The phenomenon of natural frequency and critical speed of rotating shaft is the most common problem discussed by mechanical engineers.

With the ever increasing demand for large size and velocity in modern machines, rotors dynamics become more and more important subject in the mechanical design.

The rotor bearing system contains many difficult problems such as stability, vibration characteristics and unbalance response. Consequently many researchers tried to deal with these problems, and solve them by various mathematical models.

Recent advances in computer technology have allowed more realistic, i.e., more complex, system problems to be examined as proposed to be idealized solution obtained by authors, including the static and dynamic behavior of rotating machinery which involves rotary inertia, gyroscopic moments and axial load.

Fang and Yang [1] propos a useful analysis tool for many problems in rotor dynamics, by developed a distributing transfer function synthesis for modeling and analysis of rotor systems assembled from multiple and rigid components. The method is capable of modeling flexible rigid body interactions, and the combined effect of elastic deformations, rotary inertia, unbalanced masses and gyroscopic forces.

Nelson [2] proved that the F.E.M. provides an accurate representation of rotating shaft dynamic, by utilizing shear deformation theory and F.E.M. for establishing the shape function to derive the system matrices including the effect of rotary inertia, gyroscopic moments, axial load and shear deformations.

Genta and Tonoli [3] have developed the F.E.M. for the study of the axial tensional and flexural dynamic behavior of thin rotating discs taking into account gyroscopic effect and influence of centrifugal and thermoelastic loading. The displacements within the element are assumed to be due to the superposition of its rigid body motion and the deflections relative to the rigid body configuration.

Kalkat et al [4], have designed a direct-coupled rotor system to analyze the dynamic behavior of rotating systems in regard to vibration parameters. The vibration parameters are amplitude, velocity, and acceleration in the vertical direction. The system consist of a machine analyzer, shaft, disk, master-trend software, and power unit. Four different points were detected and measured by the experimental setup. The vibration parameters were found and saved from master-trend software. These parameters were employed as the desired parameters of the network. A neural network is designed for analyzing a system's vibration parameters. The results show that the network could be used as an analyzer of such systems in experimental applications.

1. Equation of motion for Rotor

In continuum dynamics and by using the appropriate forms of potential and kinetic energies expressions, stiffness, mass and gyroscopic matrices for the element are obtained respectively, where the potential energy (PE) takes the form [3, 5].

$$PE = \frac{1}{2}\{X\}^T[K]\{X\} \tag{1}$$

The kinetic energy (KE) takes the form

$$KE = \frac{1}{2}\{\dot{X}\}^T[M]\{\dot{X}\} \tag{2}$$

And virtual work takes form

$$W_O = \{X\}^T\{Q\} \tag{3}$$

where

$[K]$ and $[M]$ are the stiffness and mass matrices respectively for the whole system which is defined as

$$[K]=[K_b]-[K_{ax}] \quad (4)$$

$$[M]=[M_{tr}]+[M_{rot}] \quad (5)$$

$\{X\}$ denotes the column vector of the nodal degree of freedom defined the complete system, and

$\{\dot{X}\}$ is the first derivative with respect to time.

$\{Q\}$ is the force vector in (N).

$[K_b]$ and $[K_{ax}]$ are the bending and axial stiffness matrices respectively in (N/m).

$[M_{tr}]$ and $[M_{rot}]$ are translation and rotary inertia mass matrices for rotor element respectively in (kg).

Applying Hamilton's principle [3, 6] gives

$$h=\int_{t1}^{t2}(KE-PE+W_O)dt \quad (6)$$

The equation of motion are thus determined by the relation

$$\int_{t1}^{t2}[\delta(KE-PE)+\delta(W_O)]=0 \quad (7)$$

The rotor element kinetic energy consists of both translational and rotational forms

$$KE=\frac{1}{2}\{\dot{q}\}^T([M_{tr}]+[M_{rot}])\{\dot{q}\}-\phi\{\dot{q}\}^T[H]\{\dot{q}\}+\frac{1}{2}*I_p\dot{\phi}^2 \quad (8)$$

where

ϕ : the spin frequency (Hz).

[H] : the matrix generated by kinetic energy equation in (Joule).

I_p : the polar mass moment of inertia in (kg m).

The potential energy of the element consists of elastic bending and energy due to axial load

$$PE=\frac{1}{2}\{q\}^T([K_b]-[K_{ax}])\{q\} \quad (9)$$

where

$\{q\}$ is generalized coordinate.

The variation work included in this study for the element is due to the distributed unbalance force

$$\partial W_O=\{\partial q\}^T(\{Q_C\}\cos\Omega t+\{Q_S\}\sin\Omega t) \quad (10)$$

where

$\{Q_c\},\{Q_s\}$ are the force vectors for $\cos\Omega t, \sin\Omega t$ direction respectively in (N).

Assuming harmonic motion of vibration and non – gyroscopic system, that is to say

$$\{\ddot{X}\}=-\Omega^2\{X\} \quad (11)$$

$$[K]\{X\}+[M]\{\ddot{X}\}=\{Q\} \quad (12)$$

where

Ω is the spin frequency in (Hz).

Then the governing equation (12) becomes

$$([K]-\Omega^2[M])\{X\}=\{Q\} \quad (13)$$

For free vibration $\{Q\}$ is a null vector and the general equation is

$[A]\{X\}=\lambda[B]\{X\}$, an eigen-value problem, can be solved to get eigen-value λ and eigen-vectors $\{X\}$ which give the corresponding mode shapes.

Disc equation

The equation of motion of the rigid disc is derived as

$$\left[M^{d}\right]\left\{\ddot{q}^{d}\right\}+\Omega\left[G_{y}^{d}\right]\left\{\dot{q}\right\}=\left\{Q^{d}\right\} \tag{14}$$

where

$[M^{d}]$: the rotary inertia mass matrix for disc in (kg) which is equal to:

$$\left[M^{d}\right]=\left[M_{tr}^{d}\right]+\left[M_{rot}^{d}\right] \tag{15}$$

$\left[G_{y}^{d}\right]$: the gyroscopic matrix for disc in (kg.m).

$\left\{Q^{d}\right\}$: the force vector for discs in (N).

Bearing equation

The generalized forces acting on the bearings can be written as

$$\left[C^{b}\right]\left\{\dot{q}\right\}+\left[K^{b}\right]\left\{q\right\}=\left\{Q^{b}\right\} \tag{16}$$

where

$[C^{b}]$: the damping matrix for bearing in (N.s/m).

$[K^{b}]$: the bearing stiffness matrix in (N/m).

$\left\{Q^{b}\right\}$: the force vector for bearing in (N).

Natural Frequency and Response Formulation

To be able to evaluate the natural frequencies equation (13) must be used, and for free vibration $\{Q\}$ must be taken as zero so

$$[K]-\lambda[M]=0 \tag{17}$$

To include gyroscopic matrix and to find gyroscopic effects on the natural frequencies, the mass and stiffness and gyroscopic matrices can be arranged as follows:

$$\left[M^{*}\right]=\begin{bmatrix} K & 0 \\ 0 & M \end{bmatrix}=\left[M^{*}\right]^{T} \tag{18}$$

$$\left[G_{y}^{*}\right]=\begin{bmatrix} 0 & -K \\ K & G_{y} \end{bmatrix}=-\left[G_{y}^{*}\right]^{T} \tag{18a}$$

$$\left[K^{*}\right]=\left[G_{y}^{*}\right]^{T}\left[M^{*}\right]^{-1}\left[G_{y}^{*}\right]=\begin{bmatrix} KM^{-1}K & KM^{-1}G_{y} \\ G_{y}^{T}M^{-1}K & K+G_{y}^{T}M^{-1}G_{y} \end{bmatrix}=\left[K^{*}\right]^{T} \tag{18b}$$

All above matrices are created to analyzeundamped gyroscopic system, because the classical modal analysis fails to produce a meaningful solution, [6, 7].

$$\left[K^{*}\right]=\lambda\left[M^{*}\right] \tag{18c}$$

$$\omega_{n}=\sqrt{\lambda} \tag{18d}$$

In order to evaluate the static response, the following equation is applied

$$[K]\{q_{t}\}=\{Q_{O}\} \tag{19}$$

Also to evaluate the unbalance response, equation (10) is used

$$\{Q\}=\{Q_{C}\}\cos\Omega t+\{Q_{S}\}\sin\Omega t \tag{20}$$

Thus a study state solution must have the same form as

$$\{q_t\} = \{q_C\}\cos\Omega t + \{q_S\}\sin\Omega t \qquad (21)$$

Then to evaluate the effect of gyroscopic matrix ($[G_y]$) of the equation of motion

$$[M]\{\ddot{q}\} - \Omega[G_y]\{\dot{q}\} + [K]\{q\} = \{Q\} \qquad (22)$$

Substituting equation (22) in equation (20) and (21) yields

$$\begin{Bmatrix} q_C \\ q_S \end{Bmatrix} = \begin{bmatrix} ([K]-\Omega^2[M]) & -\Omega^2[G_y] \\ \Omega^2[G_y] & ([K]-\Omega^2[M]) \end{bmatrix}^{-1} \begin{Bmatrix} Q_C \\ Q_S \end{Bmatrix} \qquad (23)$$

The solution of equation (23) provides the unbalance response of system [2, 5, 8].

2. Finite element programming

The beam element is one of the types that will be used to analyze the problems considered in this investigation; this element is a special case of F.E. which is called (Hierarchical F.E.), [9, 10]. The aim of this element is to increase the accuracy without the use of three-dimensional F.E. by increasing the order of polynomial equation. MATLAB 5.3 programming is a toolbox based on the finite element method designed to perform a complete study of the static and dynamic behavior of rotors. It is described to be very easy to solve all problems in this paper.Having derived the equations, it is appropriate to develop a computer package to analyze the shafts under different support conditions and with different number of carried discs placed along shafts.

The matrices are calculated and implemented in MATLAB 5.3 package. However, the following gives a summery of the subroutines function.

The analysis starts with the construction of script main file containing all the relevant data organized in the form of shape functions and parameters. The derivation and integration operations of shape functions are completed in this file. The mass, stiffness and gyroscopic matrices are assembled for any numbers of elements in this file. These matrices are transferred to other files to solve equation (17), (18c) and (23). The flow chart shown in Fig (1) illustrates the main process in the package.

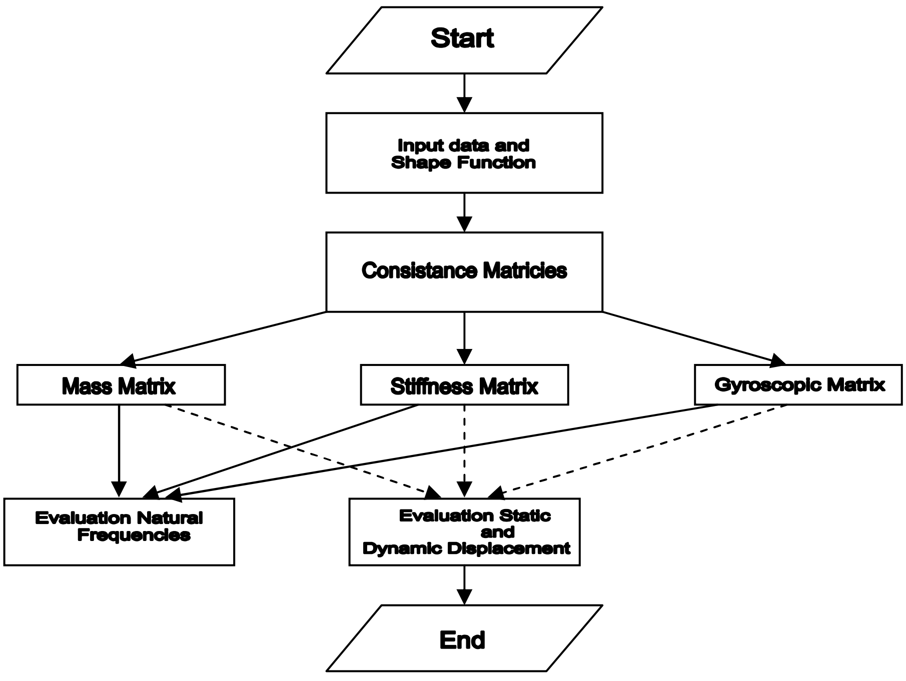

Fig (1) Flow chart of MATLAB 5.3 package

5. Experimental work

5.1 Rig description

The main purpose of designing a rig is to enable the frequency response test of a simple rotating machine to be performed to find its natural frequencies and response. Fig (2) shows the general assembly of the test rig. The test shaft with one, two, three discs and without discs in free condition is first done, then the rig with three discs are tested and supported in elastically mounted bearing and is driven by d-c motor through an elastic belt to overcome any mis-alignment. The motor is connected to speed increases and the rotor can be rotated at any speed.

The computational tools, used in this research during the rig design are the MATLAB5.3 by F.E.M. computer package which calculates the natural frequencies, mode shapes and response to system.

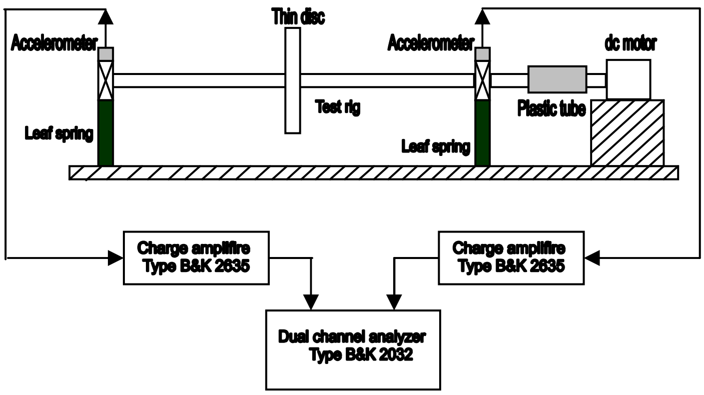

Fig (2) Schematic diagram of response test for shaft with single disc at the middle

5.2 Instrumentation [11]

The experimental apparatus used for the measurement of the free resonant frequencies and mode shapes of the test rig, are shown schematically in Fig (3) and tests are carried out under the control of the dual channel signal analyzer (type B&K 2032).

For the steady state test, as indicated by Fig (3), the control signals pass via the power amplifier (type B&K 2706) to the vibrator, regulating the frequency and amplitude. The response is measured using piezoelectric accelerometer (type B&K 4391) and charge amplifier (type B&K 2635), from which output signal are transmitted to the analyzer.

Groups of all these equipment, together with the developed test rig, perform the complete setup devices to carry out the present work are as shown in Figs (2) and (3).

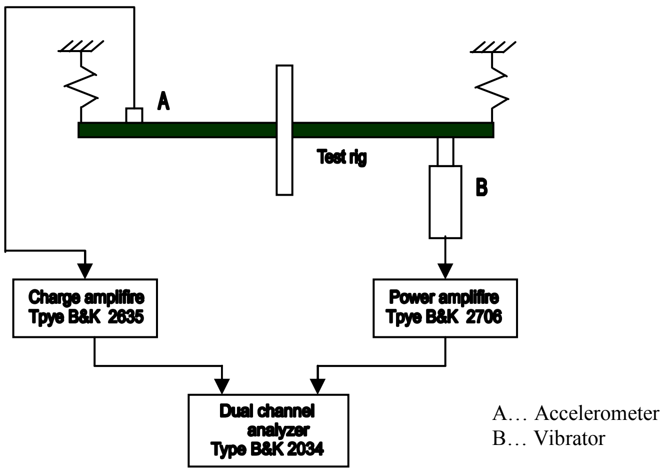

Fig (3) Free-Free natural frequencies test for shaft with single disc at the

6. The Present Results

For the static and dynamic characteristics analysis of solid shaft with different numbers of discs at various positions along the shaft, and different support condition, a computer program is developed and the present results obtained from each case are compared with the corresponding problems by other researchers. Moreover, the experimental present results are compared with theoretical ones. The results are presented as follows.

(a) Solid shaft without disc (case study one).
(b) Solid shaft with one thin disc at middle position (case study two).
(c) Solid shaft with two thin discs at the ends (case study three).
(d) Solid shaft with three thin discs two at the ends and one at middle position (case study four).

6.1 Case Study One: Shaft Without Disc

The following properties are chosen for the analysis and Fig (4a) shows shaft without disc.

$E = 2.078*10^{11}$ N/m^2	$\rho = 7806$ kg/m^3
Length of shaft = 0.4 m	d = 0.02534 m
$k_{xx} = k_{yy} = 4.378*10^7$ N/m	$k_{yx} = k_{xy} = 6*10^6$ N/m
N = 0.3	

An experimental and theoretical study is carried out on this system taking into account the effect of gyroscopic, axial load, translation and rotation inertia and bearing parameters, on the static and dynamic behavior from point of view of natural frequencies and displacement. The results obtained are compared with the other results as shown in tables (1) and (1a) and fig (5).

6.2 Case Study Two: Solid Shaft with One Thin Disc at Middle Position

The same previous properties for shaft and bearings are chosen, while the disc properties are

$m_{Disc} = 0.375$ kg $\qquad\qquad$ $d_{Disc} = 150$ mm

Fig (4b) shows the solid shaft with one thin disc at the middle position.In this study, the presence and neglecting the terms of gyroscopic, axial load, translation, rotation inertia mass and bearing stiffness effects on the natural frequencies and displacement at disc position as the spin Speed changes, as showed in Fig (6) and Tables (2), (2a).

6.3 Case Study Three: Shaft with Two Thin Discs at Ends

Fig (4c) shows the configuration of shaft with one thin disc at each end of the shaft, while the bearing are located at (0.045 m) from discs.

With this arrangement, the natural frequencies are shown in Fig (7) and Table (3), (3a) and (3b), which show the inclusion of gyroscopic forces, axial load, and translation and rotation inertia masses, all the properties of shaft, discs and bearings are same as in the last cases.

6.4 Case Study four: Shaft with Three Thin Discs

Fig (4d) shows the configuration of shaft with three thin discs. This figure differs from Fig (4c) only by the addition of another disc at the middle position of the shaft. With this arrangement, the displacement is obtained as shown in Figs (8) and (9). Table (4), (4a), (4b) and (4c) shows the inclusion of gyroscopic forces, axial load and translation and rotation inertia mass. All the properties of shaft, discs and bearings arethe same as in the last cases.

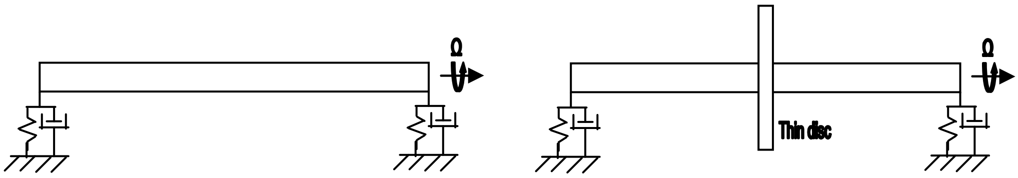

(a) Shaft without discs (case study one) (b) Shaft with one disc (case study two)

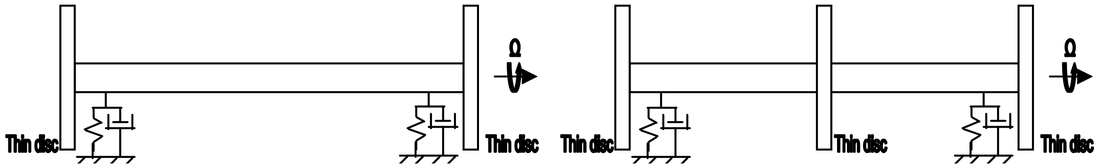

(c) Shaft with two thin discs (case study three) (d) Shaft with three discs (case study four)

Fig (4) Case studies of shafts

Table (1) Natural frequencies of shaft without thin disc

Natural frequency (Hz)	All effects & stiffness bearing (k_{xx},k_{yy}) effect	Without rotation inertia mass effects with (k_{xx},k_{yy})	Without translation inertia mass effects with (k_{xx},k_{yy})	Without gyroscopic effect with (k_{xx},k_{yy})	All effects & $(k_{xx},k_{yy},k_{xy},k_{yx})$	Free-Free theoretical	Free-Free experimental	Rayleigh Rita with (k_{xx},k_{yy})	F.E.M/R.Ritz percent %
ω_1	1903.1	1903.1	1975.36	1903.1	1746.4	0.7044	0.875	1919	0.8
ω_2	9816.93	9828.9	10185.5	9816.93	2033.28	2.1447	2.25	9920	1
ω_3	24569.7	24569.9	24753.8	24569.7	9766.14	3.977	4.375	25150.3	2.3
ω_4	40864.6	41740.6	42075	40820.9	9867.23	372.4	350	38813.3	5

Table (1a) Maximum displacement at the middle position of shaft without thin disc

Effects on rotor	All effects with (k_{xx},k_{yy})	Without gyroscopic effect with (k_{xx},k_{yy})	Without rotation inertia mass effects with (k_{xx},k_{yy})	Without translation inertia mass effects with (k_{xx},k_{yy})
Max. Displacement (mm)	0.88952	1.258	0.872	0.885

Table (2) Natural frequencies of shaft with one thin disc at middle position

Natural frequency (Hz)	All effects & stiffness bearing (k_{xx},k_{yy}) effect	Without rotation inertia mass effects with (k_{xx},k_{yy})	Without translation inertia mass effects with (k_{xx},k_{yy})	Without gyroscopic effect with (k_{xx},k_{yy})	All effects & (k_{xx},k_{yy},k_{xy},k_{yx})	Free-Free theoretical	Free-Free experimental	Rayleigh Rita with (k_{xx},k_{yy})	F.E.M/R.Ritz percent %
ω_1	1837.98	1838	1875.1	1838	1701.5	2.203	1.612	1842	0.21
ω_2	2800.6	2801	2824.5	2800.7	1966.7	4.924	5.562	2829.6	0.3
ω_3	15535.3	15558	15587.4	15535.34	2802.7	37.04	31.25	15597.8	0.4
ω_4	18987.6	19028	18562	18987.6	15464.4	384.7	358	19068	0.42

Table (2a) Maximum displacement at disc position of shaft with one thin disc at middle position

Effects on rotor	All effects with (k_{xx},k_{yy})	Without gyroscopic effect with (k_{xx},k_{yy})	Without rotation inertia mass effects with (k_{xx},k_{yy})	Without translation inertia mass effects with (k_{xx},k_{yy})
Max. Displacement (mm)	0.678	2.85	0.6884	1.042

Table (3) Natural frequencies of shaft with two thin discs at the ends

Natural frequency (Hz)	All effects & stiffness bearing (k_{xx}, k_{yy}) effect	Without rotation inertia mass effects with (k_{xx}, k_{yy})	Without translation inertia mass effects with (k_{xx}, k_{yy})	Without gyroscopic effect with (k_{xx}, k_{yy})	All effects & ($k_{xx}, k_{yy}, k_{xy}, k_{yx}$)	Free-Free theoretical	Free-Free experimental	Rayleigh Rita with (k_{xx}, k_{yy})	F.E.M/R.Ritz percent %
ω_1	536.97	536.97	537	536.97	507.12	1.267	1.046	531.8	0.9
ω_2	583	583	583	583	563	6.01	5.36	580.13	0.5
ω_3	840.12	840.12	899.2	840.13	779.54	787	750	813.7	3.1
ω_4	2954.7	2955	3003.22	2954.77	2912.4	1834	1866	3088.45	4.33

Table (3a) Maximum displacement at disc position (left disc) of shaft with two thin discs at the ends

Effects on rotor	All effects with (k_{xx}, k_{yy})	Without gyroscopic effect with (k_{xx}, k_{yy})	Without rotation inertia mass effects with (k_{xx}, k_{yy})	Without translation inertia mass effects with (k_{xx}, k_{yy})
Max. Displacement (mm)	0.973	1.12	0.8861	1.254

Table (3b) Maximum displacement at disc position (right disc) of shaft with two thin discs at the ends

Effects on rotor	All effects with (k_{xx}, k_{yy})	Without gyroscopic effect with (k_{xx}, k_{yy})	Without rotation inertia mass effects with (k_{xx}, k_{yy})	Without translation inertia mass effects with (k_{xx}, k_{yy})
Max. Displacement (mm)	0.972	1.247	0.8865	1.2527

Table (4) Natural frequencies of shaft with three thin disc, two at the ends and one at middle position

Natural frequency (Hz)	All effects & stiffness bearing (k_{xx},k_{yy}) effect	Without rotation inertia mass effects with (k_{xx},k_{yy})	Without translation inertia mass effects with (k_{xx},k_{yy})	Without gyroscopic effect with (k_{xx},k_{yy})	All effects & $(k_{xx},k_{yy},k_{xy},k_{yx})$	Free-Free theoretical	Free-Free experimental	Rayleigh Rita with (k_{xx},k_{yy})	F.E.M/R.Ritz percent %
ω_1	479.75	479.95	479.9	479.75	479.6	1.65	1	488	1.7
ω_2	505.6	505.71	506	505.6	505.61	991	970	519.8	2.73
ω_3	1301	1303	1415.5	1301	1207	2429.2	2012	1263	2.92
ω_4	2419.4	2420.2	2667.8	2419.4	1388.7	6004.15	6135	2335.8	3.45

Table (4a) Maximum displacement at disc position (left disc) of shaft with three thin discs

Effects on rotor	All effects with (k_{xx},k_{yy})	Without gyroscopic effect with (k_{xx},k_{yy})	Without rotation inertia mass effects with (k_{xx},k_{yy})	Without translation inertia mass effects with (k_{xx},k_{yy})
Max. Displacement (mm)	1.158	1.158	0.7844	0.92

Table (4b) Maximum displacement at disc position (right disc) of shaft with three thin discs

Effects on rotor	All effects with (k_{xx},k_{yy})	Without gyroscopic effect with (k_{xx},k_{yy})	Without rotation inertia mass effects with (k_{xx},k_{yy})	Without translation inertia mass effects with (k_{xx},k_{yy})
Max. Displacement (mm)	1.155	1.1588	0.784	0.918

Table (4c) Maximum displacement at disc position (middle disc) of shaft with three thin discs

Effects on rotor	All effects with (k_{xx},k_{yy})	Without gyroscopic effect with (k_{xx},k_{yy})	Without rotation inertia mass effects with (k_{xx},k_{yy})	Without translation inertia mass effects with (k_{xx},k_{yy})
Max. Displacement (mm)	1.149	1.1457	0.777	0.914

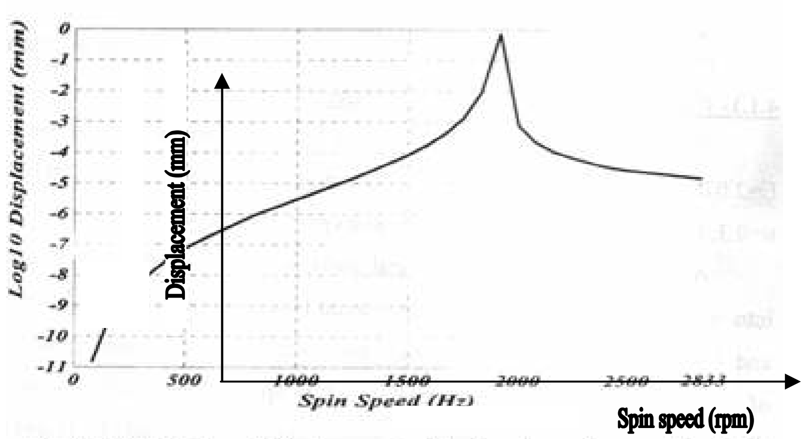

Fig (5) Variation in displacement with changing spin speed for shaft

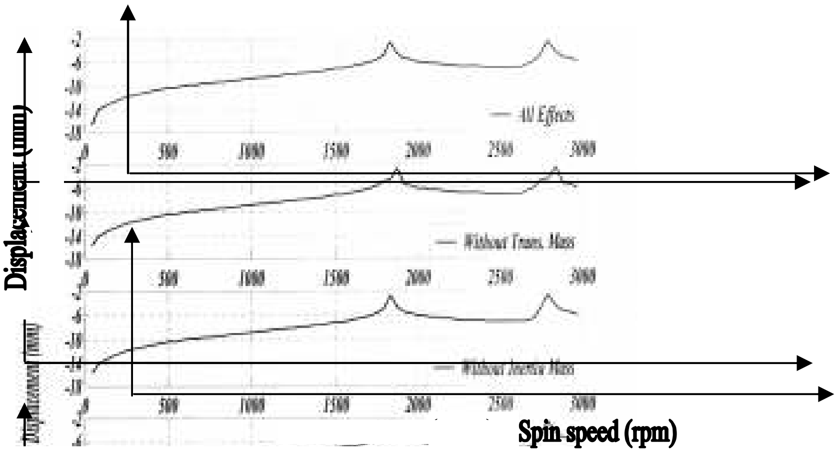

Fig (7) Variation in displacement with changing spin speed for shaft with two discs at the end

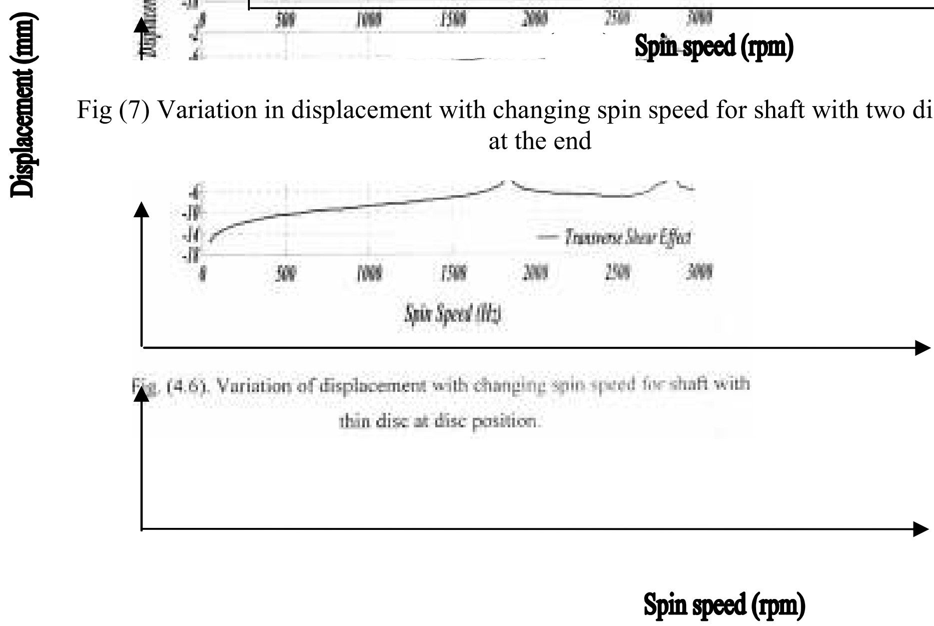

Fig (6) Variation in displacement with spin speed for shaft with thin disc at middle position

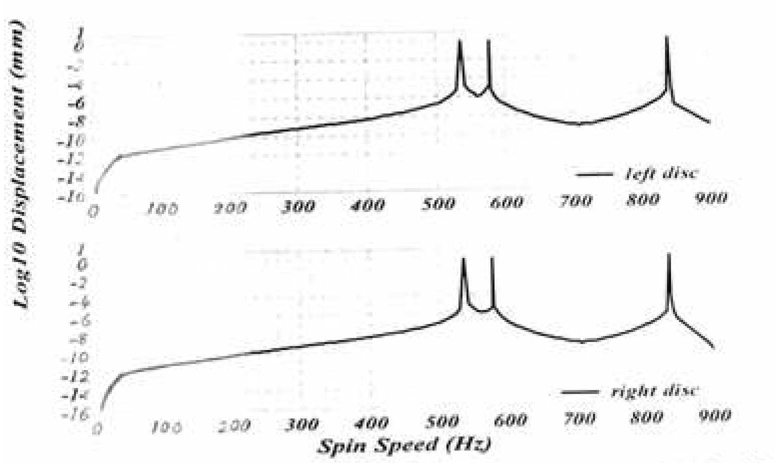

Fig. ... displacement with changing spin speed of shaft with two thin discs at the ends.

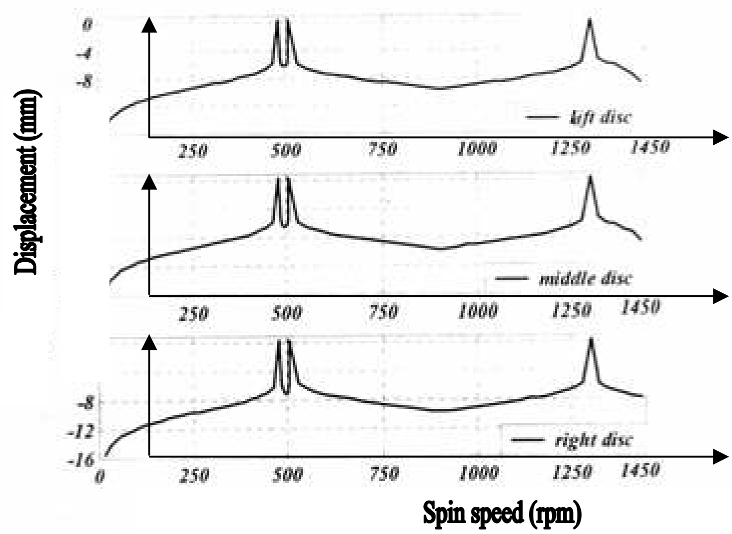

Fig (8) Variation in displacement with changing spin speed for shaft with three thin discs

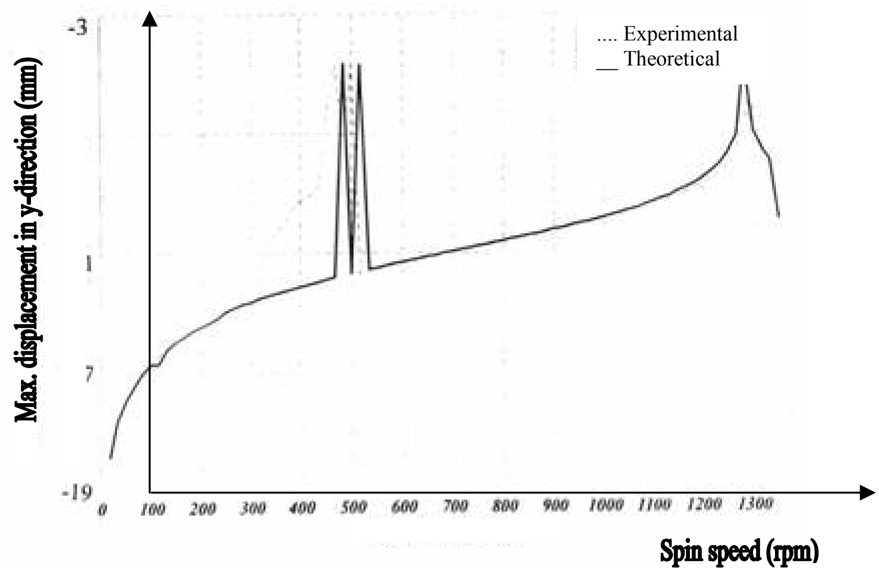

Fig (9) Variation of bearing displacement with changing spin speed of shaft with three thin discs

7. Discussions

The behavior of shaft due to the effects of combined action axial loading, gyroscopic forces and addition of single disc or multi discs along the shaft, is studied in order to obtain the variations in the displacement at disc positions and frequencies.

From Tables (1) and (2) it can be observed clearly that the presence of stiffness bearing and also the addition of stiffness components (k_{xy}, k_{yx}), cause some reduction in the natural frequencies of structures of case study one and two because of the stiffness components added to system stiffness. Moreover disc addition contributes to lower these values when cases one is compared with case two. It can be noticed that the amount of displacement (deflection) at disc position as spin speed changes, as in Fig(5), (6) and Table (1a) and (2a) in case one and two, is higher than in case three even when (k_{xy}, k_{yx}) are included, as it can be seen from Table (3). On the other hand, in case four, one can observe that this amount nearly disappears, as it can be seen clearly from Table (4). Now when discs are added at ends and middle of shaft, as shown in Fig (4c) and (4.d), case studies three and four, one can notice that the natural frequencies decrease as the number of disc increases because of the addition of disc masses.

It is observed that when the translation inertia mass effect is disregarded, the natural frequencies increase in case one and two, as shown in Tables (1) and (2), while in cases three and four this increase is quite negligible, as shown in Tables (3) and (4). Furthermore, if the rotational inertia is neglected in the above cases no noticeable changes are observed in the natural frequencies values, because the rotational inertia part is small.

An experimental study for (free-free) shaft with and without the presence of discs is carried out and the results are compared with the theoretical results obtained from this study the comparison has shown a good agreement, as shown in tables (1), (2), (3) and (4).

Tables (1a) to (4a) show the maximum displacements (deflections) values in y-directions for all cases when one of the effects mentioned earlier is neglected.

It can be noticed that the amount of displacement (deflection) at disc position changes as spin speed changes, as in Figs (5), (6) and Table (1a) and (2a) in cases one and two. Moreover, Table (3a), (3b), (4a), (4b) and (4c) show the convergence of this displacement at discs position along shaft for cases three and four, as in Figs (7) and (8) because the material is isotropic.

On the other hand, in case four the magnitude of displacement at bearing position is compared experimentally and theoretically, as shown in Fig (9) which gives a good agreement. Hence, the factors included in the theoretical consideration are quite.

8. Conclusions

From the results obtained, the following points are concluded

(1) The addition of the discs along the same shaft reduces the natural frequencies values for the different structural systems considered.

(2) The critical frequencies are convergent when the supports are placed at distance before the ends, while the designer wants the divergence between the critical frequencies.

(3) The rotational mass inertia and translational mass inertia have pronounced effect if they are neglected especially at higher modes, while the axial load and gyroscopic forces have unpronounced effect if disregarded.

(4) All the effects (rotation mass inertia, translation mass inertia, gyroscopic forces and axial load) are noticed to be necessary for studying the deformation in the systems and have a great influence on the determined values.

9. References

1. Fang H and Yang B. "Modeling Synthesis and Dynamic Analysis of Complex Flexible Rotor Systems" Journal of Sound and Vibration, Vol. 211, No. 4, pp. 571-592, 1998.
2. Nelson H D. "A Finite Rotating Shaft Element Using Timoshenko Beam Theory" Journal of Mechanical Design, Vol. 102, pp. 793-803, 1980.
3. Genta G and Tonoli A. "A Harmonic Finite Element for the Analysis of Flexural, Torsional and Axial Rotor Dynamic Behavior of Discs" Journal of Sound and Vibration, Vol. 196, No. 1, pp. 19-43, 1996.
4. Kalkat,M. Yildirim S. and . Uzmay I “Rotor Dynamics Analysis of Rotating Machine Systems Using Artificial Neural Networks” International Journal of Rotating Machinery, Vol. 9, Issue 4, pp. 255-262, 2003.
5. Archer M. and John S. “Consistent Mass Matrix for Distributed Mass System” Journal of the Structural Division, Proceedings of the ASCE, Vol. 89, ST 4, pp. 161-178, 1963.
6. Leonard M., Principles and Techniques of Vibrations, Prentice – Hall International, Inc., 1997.
7. Leonard M. “A Separation Principle for Gyroscopic Conservative Systems” *Trans.* ASME Journal of Vibration and Acoustics, Vol. 119, pp. 110-119, 1997.
8. Nelson H D and Mcvaugh J M. "The dynamics of rotor bearing system using Finite Elements" *Journal of engineering for industry*, Vol. 98, pp. 593-600, 1976.
9. Leonard M. and Baruh H. “On the inclusion principle for the Hierarchical finite element method” *Journal of numerical methods in engineering*, Vol. 19, 1983
10. Rao S., *The finite element method in engineering,* Pergamon press plc, Headington Hill Hall, 2nd edition, 1989
11. Bruel & Kjaer, “Master catalogue electronic instruments”, 1989.